Journal of Pain Research

Dovepress
open access to scientific and medical research

Open Access Full Text Article

ORIGINAL RESEARCH

Modulation of Brain Network Topological Properties in Knee Osteoarthritis by Electroacupuncture in Rats

Jun-Peng Zhang[1,*], Jun Shen[2,3,*], Yun-Ting Xiang[1,*], Xiang-Xin Xing[4], Bing-Xin Kang[5], Chi Zhao[2], Jia-Jia Wu[4], Mou-Xiong Zheng[4,6], Xu-Yun Hua[4,6], Lian-Bo Xiao[2,3], Jian-Guang Xu[1,4,7]

[1]School of Rehabilitation Science, Shanghai University of Traditional Chinese Medicine, Shanghai, People's Republic of China; [2]Department of Orthopedic, Guanghua Hospital of Integrative Chinese and Western Medicine, Shanghai, People's Republic of China; [3]Arthritis Institute of Integrated Traditional Chinese and Western Medicine, Shanghai Academy of Traditional Chinese Medicine, Shanghai University of Traditional Chinese Medicine, Shanghai, People's Republic of China; [4]Department of Rehabilitation Medicine, Yueyang Hospital of Integrated Traditional Chinese and Western Medicine, Shanghai University of Traditional Chinese Medicine, Shanghai, People's Republic of China; [5]The First Affiliated Hospital of Henan University of Chinese Medicine, Zhengzhou, People's Republic of China; [6]Department of Traumatology and Orthopedics, Yueyang Hospital of Integrated Traditional Chinese and Western Medicine, Shanghai University of Traditional Chinese Medicine, Shanghai, People's Republic of China; [7]Engineering Research Center of Traditional Chinese Medicine Intelligent Rehabilitation, Ministry of Education, Shanghai, China

*These authors contributed equally to this work

Correspondence: Jian-Guang Xu, School of Rehabilitation Science, Shanghai University of Traditional Chinese Medicine, 1200 Cailun Road, Shanghai, People's Republic of China, Email xjg@shutcm.edu.cn; Lian-Bo Xiao, Department of Orthopedic, Guanghua Hospital of Integrative Chinese and Western Medicine, 540 Xinhua Road, Changning District, Shanghai, People's Republic of China, Email xiao_lianbo@163.com

Introduction: Osteoarthritis is a chronic, ongoing disease that affects patients, and pain is considered a key factor affecting patients, but the brain changes during the development of osteoarthritis pain are currently unclear. In this study, we used electroacupuncture (EA) to intervene the rat model of knee osteoarthritis and analyzed the changes in topological properties of brain networks using graph theory.

Methods: Sixteen SD rat models of right-knee osteoarthritis with anterior cruciate ligament transection (ACLT) were randomly divided into electroacupuncture intervention group and control group. The electroacupuncture group was intervened on Zusanli (ST36) and Futu (ST32) for 20 min each time, five times a week for 3 weeks, while the control group was applied sham stimulation. Both groups were measured for pain threshold. The small-world properties and node properties of the brain network between the two groups after the intervention were statistically analyzed by graph theory methods.

Results: The differences are mainly in the changes in node attributes between the two groups, such as degree centrality, betweenness centrality, and so on in different brain regions ($P<0.05$). Both groups showed no small-world characteristics in the brain networks of the two groups. The mechanical thresholds and thermal pain thresholds were significantly higher in the EA group than in the control group ($P<0.05$).

Conclusion: The study demonstrated that electroacupuncture intervention enhanced the activity of nodes related to pain circuit and relieved pain in osteoarthritis, which provides a complementary basis for explaining the effect of electroacupuncture intervention on pain through graphical analysis of changes in brain network topological properties and helps to develop an imaging model for pain affected by electroacupuncture.

Keywords: osteoarthritis, electroacupuncture, pain, spatio-temporal analysis, neural plasticity

Introduction

Osteoarthritis (OA) places a progressively increasing burden on the health of individuals and the economic cost to society, influenced by an aging population and an increasing obese population.[1,2] More than 240 million people worldwide suffer from osteoarthritis, and 30% of people over 45 years old have been diagnosed with imaging features of osteoarthritis of the knee.[3] Osteoarthritis is a disease where joint damage fails to repair due to abnormal stress on any

Received: 13 February 2023
Accepted: 2 May 2023
Published: 17 May 2023

joint or peri-articular tissue. The disease is known to have complex pathophysiology that affects multiple joints and joint structures.[4] Currently, osteoarthritis is considered to be a disease of the whole joint, including alterations in the articular cartilage, subchondral bone, ligaments, capsule, and synovial membrane, ultimately leading to joint failure.[5] Pain, stiffness, decreased joint motion and muscle weakness are signs and symptoms of osteoarthritis of the knee.[3] The effects of a patient suffering from long-term knee osteoarthritis may include reduced physical activity, decreased physical function, impaired sleep, fatigue, depression, and disability. The severity of symptoms and structural damage on imaging are often inconsistent.[4]

Pain is considered to be key for patients affected by osteoarthritis, OA pain leads to significant limitations in joint function and reduced quality of life.[6] Previous magnetic resonance imaging (MRI) studies have found that the severity of structural osteoarthritis is moderately correlated with joint pain and is associated with specific features of osteoarthritis, such as the size and number of bone marrow lesions and synovitis.[2] Pain sensitization is an abnormal response caused by changes in nociceptive processing in the peripheral or central nervous system.[7] Pain relief treatments, especially for the treatment or prevention of sensitive pain, are critical in the future. Based on the current evidence, it appears that pain in OA may be driven by nociceptive and neuropathic mechanisms.[2] Nociceptive mechanisms are mainly caused by the increased reactivity of peripheral nociceptors due to continuous tissue damage or inflammation within the joint. However, the neural pathophysiological mechanisms of osteoarthritis are still not clear enough, so one of the major issues in the current treatment of osteoarthritis is to explore the brain changes caused by osteoarthritis, only by clarifying the corresponding mechanisms can targeted treatments be developed.

According to a recent study, abnormal activation of multiple brain regions is associated with osteoarthritis pain in rats when studying brain function in rats with osteoarthritis, including somatosensory cortex, insula, anterior cingulate cortex (ACC), thalamus, amygdala, nucleus ambiguous cortex (NAC), hippocampus and periaqueductal gray matter (PAG) of the midbrain, which are all associated with pain processing, reward and emotion.[8] In addition, some researchers have also found that the network topology of the brain at rest affects the degree of pain modulation that occurs in subsequent experiments, reflecting the fact that topological network properties predict adaptive responses to environmental influences.[9] However, there is still a lack of research on the topological properties of brain networks in osteoarthritis.

The clinical effectiveness of traditional Chinese medicine acupuncture treatment has been demonstrated in several large, high-quality randomized controlled trials.[10,11] Previous studies have shown that patients with knee osteoarthritis who have received acupuncture treatment have a significant improvement in pain and joint function compared to those who do not receive acupuncture treatment.[12] Patients with chronic pain are increasingly using acupuncture for pain relief.[13,14]

As the human brain is one of the most complex systems, we adopted a brain network analysis approach to study the complex structural network of connections and the functional network of interactions constituted by microscopic neurons or macroscopic brain regions.[15] While traditional network science tools can provide a basic characterization of brain function, they are usually unable to identify pathophysiological mechanisms or to link system-level phenotypes to multiple levels of brain function.

The use of graph theoretic methods to characterize the topological relationships of complex networks is an important tool for us to study the overall properties of different nodes, different connected edges, and different networks in complex networks.[16]

The more consistent findings of experiments using a graph-theoretic approach on the neural basis of different diseases suggest that this approach holds great promise for a comprehensive and sustainable model in future functional magnetic resonance imaging (fMRI) studies.[17] By constructing static, dynamic, and multimodal brain networks and analyzing graph theoretic metrics, we are able to study complex networks further. These changes in network topology may predict different functional impairments and help us to understand the relationship between different functional brain networks better.[18]

Previous studies have found that continuous electroacupuncture (EA) intervention in patients with knee osteoarthritis significantly reduced the regional coherence of pain-related brain regions, and there is an expectation that the analgesic effect of electroacupuncture intervention can be predicted by analysis of brain networks.[19,20] Therefore, this study aims to explore the corresponding mechanisms through the analysis of magnetic resonance imaging results using a rat model

of knee osteoarthritis. Based on the experience of other researchers, the Zusanli (ST36) and the Futu (ST32) are commonly used acupoints for treating knee osteoarthritis. Therefore, this study will also use these two acupoints as intervention points.[10,21,22]

Consequently, we choose to analyze the altered topological properties of the resting-state brain network in rats after electroacupuncture intervention for knee osteoarthritis using graph theory.

Methods

Animals

Adult female Sprague-Dawley (SD) rats (weight 180–200 g) were obtained from Guanghua Hospital, Shanghai University of Traditional Chinese Medicine. All animal experiments were approved by the Animal Ethics Committee of Guanghua Hospital, Shanghai University of Traditional Chinese Medicine, and performed in compliance with the National Institutes of Health Guide for the Care and Use of Laboratory Animals (2022-K-30). All rats lived in individual plastic ventilated cages in an environment with an ambient temperature of about 24 degree Celsius, a light–dark cycle of 12 h, and an adequate supply of food and water.

Experimental Procedure

In this experiment, the anterior cruciate ligament transection (ACLT) rat model of osteoarthritis of the right knee was used.[23] Rats were anesthetized by intraperitoneal injection of sodium pentobarbital (40 mg/kg) until they had shallow and slow respiration, limb weakness, and diminished or absent corneal reflexes. The right hind limb was then shaved and prepared for aseptic surgery. The rat was secured in a supine position on a surgical table with a routine iodophor sterilized layette. A 1.5 cm incision was made above the rat's knee joint, and then the superficial fascial tissue and joint capsule were exposed using a medial parapatellar approach, and the patella was retracted laterally with the knee fully extended, then the joint was returned to full flexion. At this point, the anterior cruciate ligament (ACL) was transected with microscissors under the surgical microscope. After rinsing with saline to remove tissue debris, the skin incision was sutured.

A total of 16 rats were randomly divided into two groups, one for the electroacupuncture intervention group and one for the sham stimulation group (control). After 7 days of modeling, the intervention was performed on the EA group. After the rats were fixed during the intervention period, disposable sterile acupuncture needles (φ0.25 mm × 40 mm) were used to pierce the Zusanli (ST36) and the Futu (ST32) on the hind limb of the healthy side, as shown in Figure 1, with the Zusanli located on the lateral side of the tibial tuberosity and the Futu located on the tibialis anterior muscle below the knee joint, and the piercing depth was 5 mm.[21,22] The two needles were then connected to the electrical stimulator (Huatuo SDZ-V nerve and muscle stimulator, Suzhou Medical Appliance Factory, Suzhou, China). The EA parameters were set as follows: dense disperse waves of 2 Hz; 0.2 ms pulse width, 2 mA intensity for 20 min/day, 5 times per week for 3 weeks.

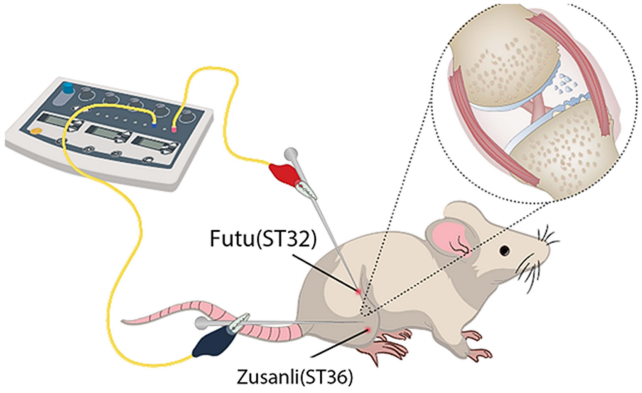

Figure 1 Schematic diagram indicates the two selected acupoints, Zusanli (ST36) and Futu (ST32), which correspond to equivalent acupoints in humans.

In the sham stimulation group, disposable sterile acupuncture needles (φ0.25 mm × 40 mm) were used to pierce the Zusanli (ST36) and the Futu (ST32) on the hind limb of the healthy side, but the connected electroacupuncture instrument was not given electrical stimulation pulses, which were maintained for 20 min once a day, 5 days a week, for 3 weeks.

Behavioral Tests

The behavioral tests were collected at baseline before modeling, and the results were collected after the intervention was completed.

Mechanical threshold collection:[24] Rats were placed in separate transparent squares and allowed to acclimatize to the environment for 30 min. Afterwards, the rats were free from washing and scratching and remained quiet. The posterior plantar region of the rat's postoperative limb was stimulated by using a Von-Frey filaments with bending forces of 4 g, 8 g, and 15 g, respectively, five times for 5 s each. Rats were counted as positive for sudden foot lift, foot licking, or foot lift after removal of filaments, and this was then expressed using overall percentages.

Thermal pain threshold collection:[25] We measured the thermal pain threshold in rats using a removable thermal radiometric pain meter. Firstly, the rats were placed in an organic plastic container on a transparent glass plate of the thermal radiometric pain meter and allowed to acclimatize for 30 min. After the rats were quiet, the plantar surface of the rats was irradiated using the thermal radiometric pain meter, and the thermal stimulation intensity of the pain meter was set to 30%, and the maximum time was set to 30 s to avoid burns. When the rat's hind foot was burning pain, it lifted the hind foot quickly. At this time, the time from the beginning of pain measurement to the rat's hind foot lifting will appear on the thermal radiation pain meter, and the thermal stimulation contraction reflex time will be recorded accurately, and each rat will be tested 3 times with 5 min interruption each time. The values were noted, and the mean value was obtained as the thermal pain threshold.

fMRI Acquisition and Preprocessing

Functional MRI was given to rats after 3 weeks of intervention. All fMRI data were collected by a 7-T horizontal-bore Bruker scanner (Bruker Corporation, Ettlingen, Germany) with a gradient system of 116 mm inner diameter and 400 mT/m maximum gradient strength.[26,27] Rats were anesthetized initially with 4% isoflurane and then fixed on the scanner and maintained with 1.5–2% isoflurane in oxygen-enriched air (20% oxygen/80% air) with necessary ventilator support. fMRI images were acquired using a Gradient Echo-Echo Planar Imaging (GRE-EPI) sequence with the following parameters: interleaved scanning order; Field of view = 32 × 32 mm^2; matrix size = 64 × 64; slice number = 43; Time of repetition/echo = 3000/20 ms; flip angle = 90°; slice thickness = 0.5 mm;

fMRI data were corrected for upscaling (magnification 10×), stripping none-brain tissue, reorientation, slice-timing, realignment, coregistration, spatially warped and resampled to the template in MNI space, and spatially smoothed with an isotropic Gaussian kernel (full width at half maximum) twice as the voxel size.

Brain Network Analysis and Statistical Analysis

GRETNA was used to construct a functional brain network.[28] Based on MNI-supported anatomical automatic labeling (AAL), the software divided the entire cerebral cortex into 90 cortical and subcortical anatomically defined regions. In addition, the mean time series of each region was extracted. We then calculated Pearson's correlation coefficients for each pair of regions in AAL and used Fisher's z transformation to convert the data to z-values close to a normal distribution. A binary connection matrix converted by the z-values with a selected threshold of the relation matrix was used to construct a graphical model of the functional network. Our sparsity was set to 0.05–0.5 with an interval of 0.01 based on previous studies. We used the GRETNA to calculate the topological properties in the network, and the following metrics represent the global characteristics of the functional network: clustering coefficient (Cp), characteristic path length (Lp), Normalized clustering coefficients (γ), Normalized characteristic path length (λ) and Small worldness (σ). We used Betweenness Centrality, Degree Centrality (DC), Nodal cluster coefficiency, Nodal Efficiency, Nodal local efficiency, and Nodal shortest path to demonstrate the nodal properties in the functional network.

Behavioral Data Statistical Analysis

IBM SPSS Statistics 25 was used for statistical analysis, and data were expressed as mean ± standard deviation (Mean ± SD). Pain behavioral data were analyzed using a two-sample *t*-test. $p<0.05$ was considered a statistically significant difference. Furthermore, Pearson correlation analysis was performed between the extracted meaningful brain region t-values and the thermal withdrawal threshold as well as the Von-Frey threshold.

Results

Pain Threshold

After 3 weeks of intervention, both mechanical and thermal pain thresholds in the EA group were significantly higher than those in the control group (Figure 2), and lower values indicate more severe pain, $p<0.001$.

Nodal Characteristics in the Functional Networks

Comparing the nodal characteristics of the EA group with the control group in the resting state (Table 1, Figure 3), the Betweenness Centrality in the EA group showed a decrease in the right ventral tegmental area (VTA) and an increase in the left interstitial nucleus of the posterior limb of the anterior commissure (IPAC) compared with the control group. Degree Centrality decreased in the bilateral subiculum hippocampus, right cingulate cortex, right ventral hippocampus, left posterior hippocampus, and increased in the left Globus Pallidus, lateral hypothalamus, left internal capsule, and left IPAC in the EA group compared to the control group. Nodal cluster coefficient showed a decrease in the right subiculum hippocampus and an increase in the left globus pallidus and left internal capsule in EA group compared to the control group. Nodal efficiency of the EA group was lower in the right cingulate cortex, left subiculum hippocampus, left posterior hippocampus, and left medial geniculate, and higher in the left auditory cortex, lateral hypothalamus, internal capsule, and IPAC compared to the control group. Nodal local efficiency in the EA group demonstrated a decrease in the right subiculum hippocampus and the left posterior hippocampus, and an increase in the left internal capsule and globus pallidus compared to the control group. The nodal shortest path of the EA group showed an increase in the bilateral cingulate cortex and a decrease in the left auditory cortex compared with the control group.

Small Worldness

Figure 4 shows the comparison of the small-world parameters of the whole-brain network between the EA group and the control group in the resting state, and the measured sparsity ranges from 0.05 to 0.5.

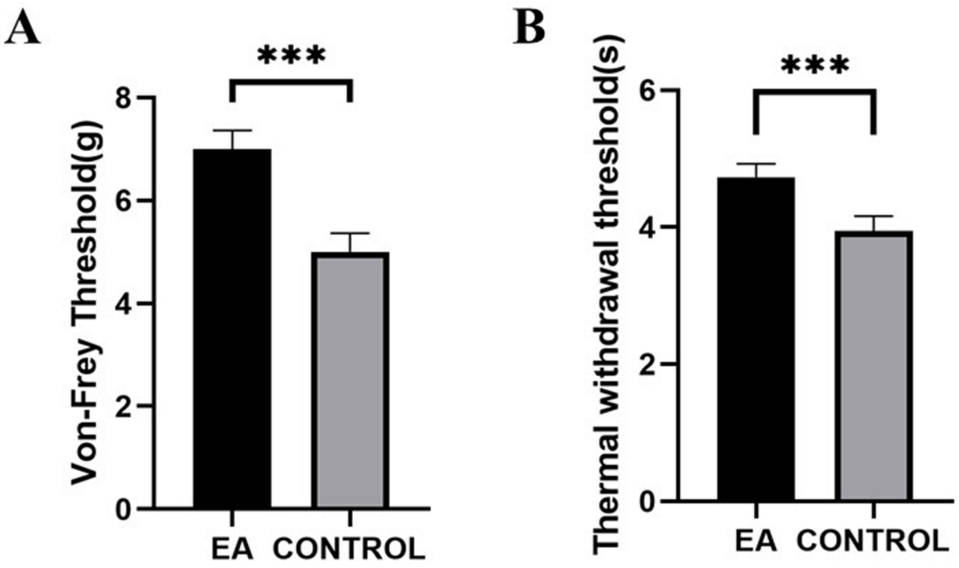

Figure 2 Pain thresholds after three weeks of intervention.
Notes: (**A**) Mechanical threshold, (**B**) thermal pain threshold; ***p<0.0001.

Table 1 Brain Regions with Significant Nodal Characteristic Between EA Group and Control Group

Nodal Characteristic	Brain Region	P	t
Betweenness Centrality	R_VTA	0.007	−3.417
	L_IPAC	0.012	3.079
Degree Centrality	R_Cortex_Cingulate	0.034	−2.462
	R_Hippocampus_Subiculum	0.031	−2.508
	R_Hippocampus_Ventral	0.009	−3.259
	L_Globus_Pallidus	0.020	2.770
	L_Hippocampus_Posterior	0.002	−4.289
	L_Hippocampus_Subiculum	0.004	−3.739
	L_Hypothalamus_Lateral	0.039	2.374
	L_IC	0.001	4.347
	L_IPAC	0.003	3.956
Nodal cluster coefficiency	R_Hippocampus_Subiculum	0.046	−2.277
	L_Globus_Pallidus	0.026	2.604
	L_IC	0.001	4.615
Nodal Efficiency	R_Cortex_Cingulate	0.018	−2.822
	L_Cortex_Auditory	0.013	3.014
	L_Hippocampus_Posterior	0.004	−3.692
	L_Hippocampus_Subiculum	0.006	−3.464
	L_Hypothalamus_Lateral	0.047	2.264
	L_IC	0.006	3.522
	L_IPAC	0.005	3.554
	L_Medial_Geniculate	0.042	−2.337
Nodal local efficiency	R_Hippocampus_Subiculum	0.010	−3.196
	L_Globus_Pallidus	0.022	2.711
	L_Hippocampus_Posterior	0.014	−2.983
	L_IC	0.001	4.528
Nodal shortest path	R_Cortex_Cingulate	0.016	2.882
	L_Cortex_Auditory	0.030	−2.521
	L_Cortex_Cingulate	0.035	2.430

Note: $p<0.05$, uncorrected.
Abbreviations: VTA, ventral tegmental area; IPAC, interstitial nucleus of the posterior limb of the anterior commissure; IC, internal capsule; R, right; L, left.

After comparing the clustering coefficient and characteristic path length of the two groups, the results showed no statistical difference ($p>0.05$). After comparing the Normalized clustering coefficients (γ) and Normalized characteristic path length (λ) of EA group and control group, we find that there is no statistical difference between them ($p>0.05$), and the small-world coefficient σ is obtained by substituting the formula $\sigma=\gamma/\lambda$, and we get $\sigma\approx1$ ($p>0.05$), the results show that the functional network does not have the small-world property.

Correlations

Through correlation analysis between all meaningful indicators and the Von-Frey threshold of the thermal withdrawal threshold, it was found that in the control group, there was a significant correlation between the Von-Frey threshold and the DC of left subiculum hippocampus ($p=0.045$); there was also a significant correlation between the thermal withdrawal threshold and the DC of left subiculum hippocampus ($p=0.0447$). In the EA group, there was a significant correlation between the thermal withdrawal threshold and the nodal shortest path of right cingulate cortex ($p=0.0218$).

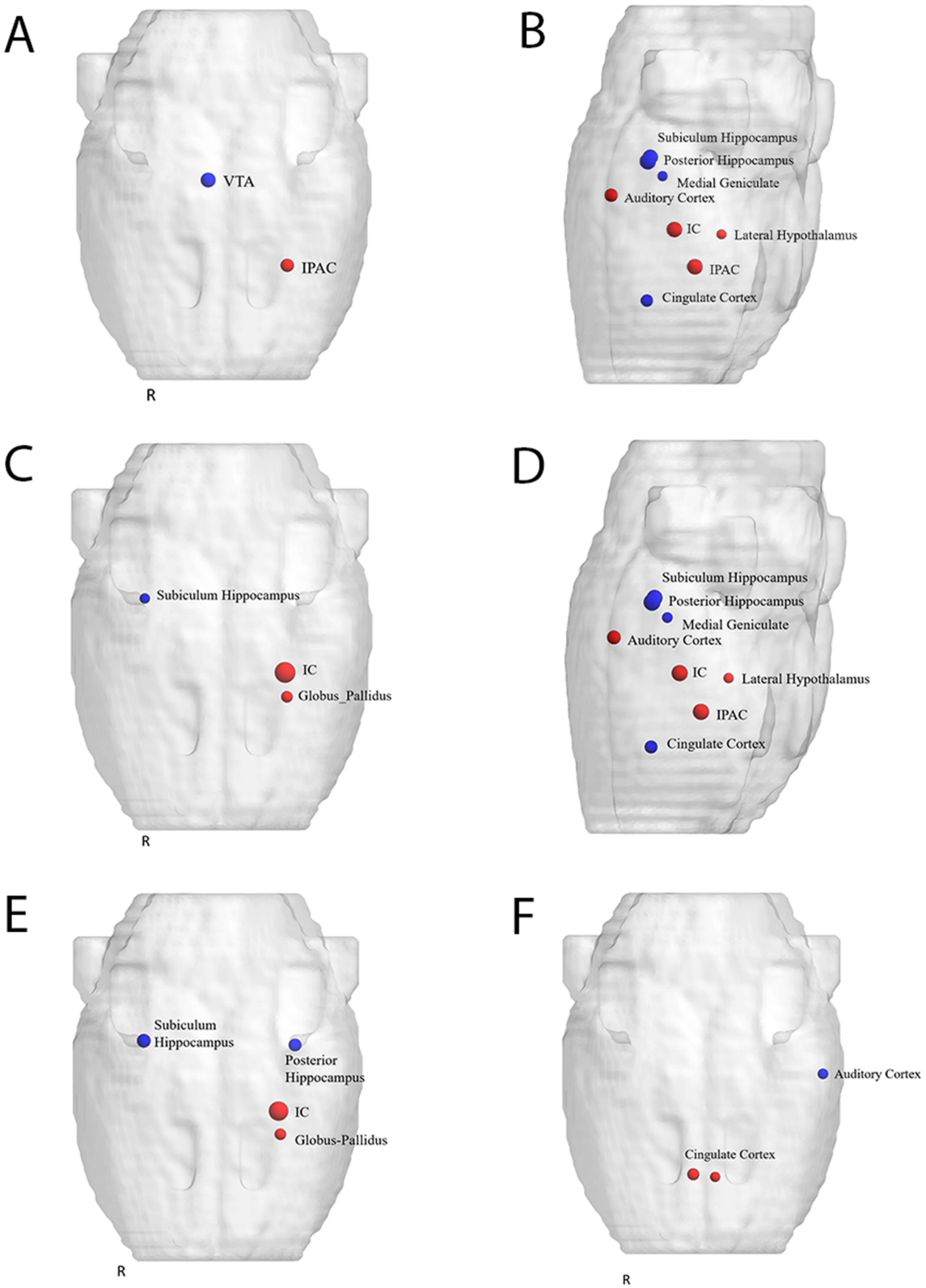

Figure 3 The nodal parameters of the global cerebral resting-state functional network between EA group and control group.
Notes: (**A**) Betweenness centrality, (**B**) degree centrality (DC), (**C**) nodal cluster coefficiency, (**D**) nodal efficiency, (**E**) nodal local efficiency, and (**F**) nodal shortest path; The red ball represents increased value of nodal properties, while the blue balls represent decreased. The size of ball represents a significant difference; $p<0.05$, uncorrected.

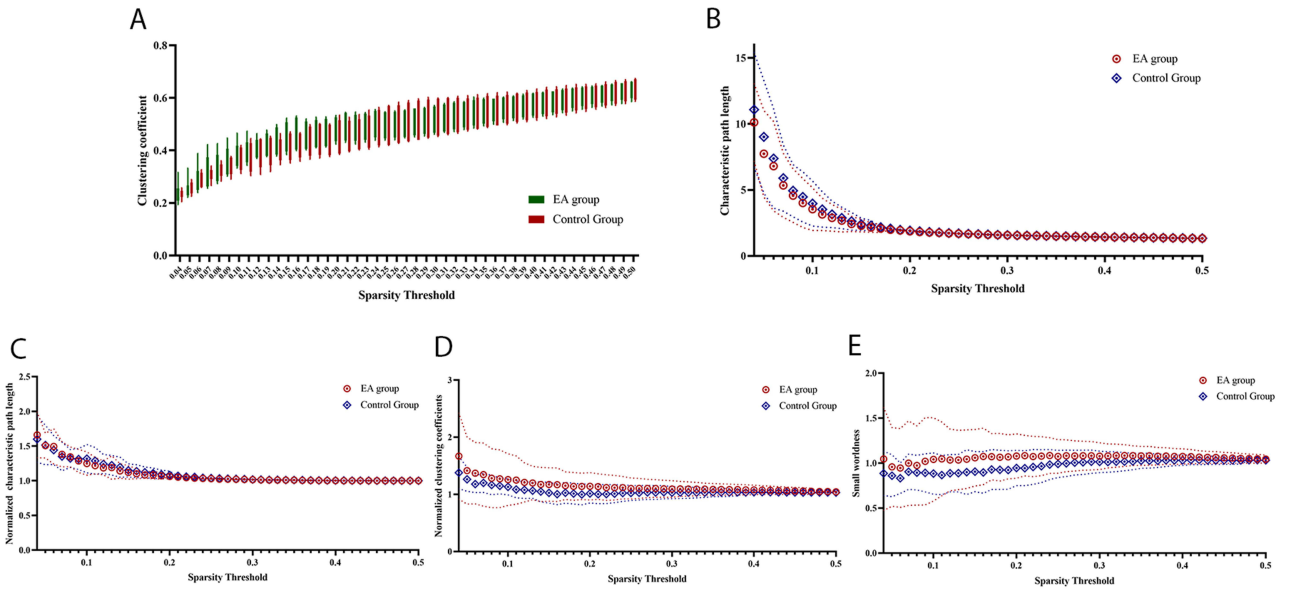

Figure 4 The small-world parameters of the global cerebral resting-state functional network between EA group and control group at a sparsity range of 0.05–0.5.
Notes: (**A**) Clustering coefficient, (**B**) characteristic path length, (**C**) normalized clustering coefficients (γ), (**D**) normalized characteristic path length (λ), (**E**) small worldness (σ); P>0.05.

Discussion

In this study, the changes in the topological properties of brain networks of rat models after electroacupuncture intervention for knee osteoarthritis were analyzed for the first time using a graph-theoretic approach. This study found that the differences in topological properties between the electroacupuncture intervention group and the sham stimulation group mainly focused on the nodal properties, and there were no differences in the small-world properties. Node properties were used as a criterion to determine the importance of the node in the network, and we further clarified the effect of the electroacupuncture intervention on the brain network compared to the sham stimulation by analyzing the node properties.

IPAC receives input from several autonomic/limbic regions of the forebrain, including the agranular insular cortex, bed nucleus of the stria terminalis, the amygdaloid complex, and the lateral hypothalamic area.[29] The IPAC is intermediate between both the ventral striatal pallid nucleus system and the extended amygdala system, is directly connected to the caudal nucleus of the vomeronasal nucleus, and is connected caudally to the central amygdala, and studies suggest that the IPAC is one of the important parts involved in the regulation of the autonomic nervous system.[30] Studies have confirmed that the IPAC receives direct projections from the VTA and NAC, but its exact fine loop structure remains unclear.[31] There is a lack of functional verification of the IPAC, but some scholars have inferred that it may be involved in emotions, drug addiction, and other related processes based on its morphology and connections with other brain regions.[29] In addition, dopaminergic neurons in the VTA of the midbrain are thought to be critical in the regulation of various psychoactive substance-mediated rewarding effects.[32]

Betweenness Centrality, as a measure of the connectivity between different nodes connected at a given node, was increased in the electroacupuncture group in the left IPAC, and decreased in the right VTA, possibly indicating a left VTA-IPAC circuit activation. This change was matched by behavioral findings that the pain threshold in the EA group was significantly higher than the sham stimulation in the control group, which could laterally respond to the relief of pain caused by osteoarthritis with a long-term electroacupuncture intervention facilitating the activation of the related reward circuits.

Degree centrality is the most direct measure of the centrality of a node in network analysis.[33] A greater nodal degree of a node means that the node is more important in the network. In the comparison of the present study, the EA group was found to have increased degree centrality in the left pallidum, the lateral part of the hippocampus, the internal

capsule, and IPAC, suggesting the involvement of limbic circuits and sensory networks. Similar results were shown in the nodal efficiency results. Based on a large number of brain imaging studies, a consensus has emerged that the origin of pain is not limited to a single region, but rather that pain is the result of an integrated function across brain networks.[34] For example, key components of the limbic circuitry: the amygdala, cingulate cortex, hippocampus, ventral striatum, and medial prefrontal cortex, are the brain regions that govern emotion, expectancy, and salience.[35] Limbic circuits play a key role in the emotional regulation of pain.[36] Previous studies have suggested that the modulation of pain circuit by acupuncture may be designed to lead to alterations in dopamine activity and involve reward circuits, possibly due to altered brain adaptations resulting from the persistent injury of knee osteoarthritis.[37]

In this study, a significant decrease in degree centrality and nodal efficiency was observed in the right cingulate cortex. Nodal shortest path in the left cingulate cortex increased, while the pain threshold on the affected side also appeared significantly elevated, and the anterior cingulate gyrus, which is a central part of the reward circuit, may reflect the activation of the reward circuit by electroacupuncture from the inhibition of pain, reducing the transmission of pain to the center from the source of pain. At the same time, we also found that electroacupuncture intervention significantly alleviated pain in rats with knee osteoarthritis. This study can help us further understand the brain network mechanisms of electroacupuncture intervention in a rat model of knee osteoarthritis, providing theoretical support for clinical electroacupuncture intervention in knee osteoarthritis.

These results did not show a change in small-world properties, which may be related to the size of the sample size. By the same token, this result did not mean that the connectivity of these pathways did not change, because although we consider structural pathways as the basis of functional connectivity patterns, but the current findings suggest that there is no one-to-one correspondence between topological properties in functional and structural organization.[38,39] For example, in some neurological disorders such as schizophrenia, small-world network abnormalities may even show opposite directions in functional and structural organization.[40] This requires an in-depth study of structure–function relationships to help elucidate the deviations in functional and structural graphical indicators found in these studies for future work.

The limitations of this study mainly have two aspects: (1) Limited sample size: Due to the high cost of small animal MRI, the number of samples included in the study is relatively small. This may affect the reliability and generalizability of the study. (2) Lack of other tests: This study only used behavioral and imaging tests to evaluate changes in rat osteoarthritis but did not perform pathological tests on the tissues around the knee joint. Therefore, there is a lack of comprehensive understanding of the impact of knee joint disease on rats.

Conclusion

This study further clarified that the changes in topological properties of brain networks in rats after electroacupuncture intervention against osteoarthritis were mainly concentrated in pain-related brain network nodes and relieved pain in osteoarthritis, as well as that electroacupuncture relieved pain in osteoarthritis and had activation of the reward circuit. This provided a basis for further clarifying brain changes during osteoarthritis pain and provided a supplementary basis for explaining the effect of electroacupuncture intervention on pain by graphical analysis of topological properties of brain networks and helps to develop an imaging model for pain affected by electroacupuncture.

Informed Consent

All protocols and procedures followed the guidelines of the Biomedical Resource Center and were approved by the Animal Ethical Committee of Guanghua Hospital of Integrative Chinese and Western Medicine.

Funding

This work was supported by Shanghai Science and Technology Committee [Grant No.: 21Y11921500; Grant No.:22Y11923200; Grant No.:22ZR1453000]; three-year action plan of shanghai traditional Chinese medicine [Grant No.: ZY (2021-2023)-0201-06]; shanghai municipal health commission [Grant No.: 202140163].

Disclosure

The authors declare that they have no conflicts of interest in this work.

References

1. Bortoluzzi A, Furini F, Scirè CA. Osteoarthritis and its management - epidemiology, nutritional aspects and environmental factors. *Autoimmun Rev*. 2018;17(11):1097–1104. doi:10.1016/j.autrev.2018.06.002
2. Hunter DJ, Bierma-Zeinstra S. Osteoarthritis. *Lancet*. 2019;393(10182):1745–1759. doi:10.1016/s0140-6736(19)30417-9
3. Katz JN, Arant KR, Loeser RF. Diagnosis and treatment of hip and knee osteoarthritis: a review. *JAMA*. 2021;325(6):568–578. doi:10.1001/jama.2020.22171
4. Sharma L. Osteoarthritis of the knee. *N Engl J Med*. 2021;384(1):51–59. doi:10.1056/NEJMcp1903768
5. Martel-Pelletier J, Barr AJ, Cicuttini FM, et al. Osteoarthritis. *Nat Rev Dis Primers*. 2016;2:16072. doi:10.1038/nrdp.2016.72
6. Yu H, Huang T, Lu WW, Tong L, Chen D. Osteoarthritis Pain. *Int J Mol Sci*. 2022;23(9). doi:10.3390/ijms23094642
7. Vina ER, Kwoh CK. Epidemiology of osteoarthritis: literature update. *Curr Opin Rheumatol*. 2018;30(2):160–167. doi:10.1097/BOR.0000000000000479
8. Da Silva JT, Tricou C, Zhang Y, Tofighbakhsh A, Seminowicz DA, Ro JY. Pain modulatory network is influenced by sex and age in a healthy state and during osteoarthritis progression in rats. *Aging Cell*. 2021;20(2):e13292. doi:10.1111/acel.13292
9. Tetreault P, Mansour A, Vachon-Presseau E, Schnitzer TJ, Apkarian AV, Baliki MN. Brain connectivity predicts placebo response across chronic pain clinical trials. *PLoS Biol*. 2016;14(10):e1002570. doi:10.1371/journal.pbio.1002570
10. Lin LL, Tu JF, Wang LQ, et al. Acupuncture of different treatment frequencies in knee osteoarthritis: a pilot randomised controlled trial. *Pain*. 2020;161(11):2532–2538. doi:10.1097/j.pain.0000000000001940
11. Boutron I, Tubach F, Giraudeau B, Ravaud P. Methodological differences in clinical trials evaluating nonpharmacological and pharmacological treatments of hip and knee osteoarthritis. *JAMA*. 2003;290(8):1062–1070. doi:10.1001/jama.290.8.1062
12. Chen AT, Shrestha S, Collins JE, Sullivan JK, Losina E, Katz JN. Estimating contextual effect in nonpharmacological therapies for pain in knee osteoarthritis: a systematic analytic review. *Osteoarthritis Cartilage*. 2020;28(9):1154–1169. doi:10.1016/j.joca.2020.05.007
13. Li J, Li YX, Luo LJ, et al. The effectiveness and safety of acupuncture for knee osteoarthritis: an overview of systematic reviews. *Medicine*. 2019;98(28):e16301. doi:10.1097/MD.0000000000016301
14. Corbett MS, Rice SJ, Madurasinghe V, et al. Acupuncture and other physical treatments for the relief of pain due to osteoarthritis of the knee: network meta-analysis. *Osteoarthritis Cartilage*. 2013;21(9):1290–1298. doi:10.1016/j.joca.2013.05.007
15. Luo L. Architectures of neuronal circuits. *Science*. 2021;373(6559):eabg7285. doi:10.1126/science.abg7285
16. Bullmore E, Sporns O. Complex brain networks: graph theoretical analysis of structural and functional systems. *Nat Rev Neurosci*. 2009;10(3):186–198. doi:10.1038/nrn2575
17. Medaglia JD. Graph theoretic analysis of resting state functional MR imaging. *Neuroimaging Clin N Am*. 2017;27(4):593–607. doi:10.1016/j.nic.2017.06.008
18. van den Heuvel MP, Hulshoff Pol HE. Exploring the brain network: a review on resting-state fMRI functional connectivity. *Eur Neuropsychopharmacol*. 2010;20(8):519–534. doi:10.1016/j.euroneuro.2010.03.008
19. Gollub RL, Kirsch I, Maleki N, et al. A functional neuroimaging study of expectancy effects on pain response in patients with knee osteoarthritis. *J Pain*. 2018;19(5):515–527. doi:10.1016/j.jpain.2017.12.260
20. Tu JF, Yang JW, Shi GX, et al. Efficacy of intensive acupuncture versus sham acupuncture in knee osteoarthritis: a randomized controlled trial. *Arthritis Rheumatol*. 2021;73(3):448–458. doi:10.1002/art.41584
21. He TF, Yang WJ, Zhang SH, Zhang CY, Li LB, Chen YF. Electroacupuncture inhibits inflammation reaction by upregulating vasoactive intestinal peptide in rats with adjuvant-induced arthritis. *Evid Based Complement Alternat Med*. 2011;2011:1–8. doi:10.1155/2011/290489
22. Huang CH, Yeh ML, Chen FP, Wu D. Low-level laser acupuncture reduces postoperative pain and morphine consumption in older patients with total knee arthroplasty: a randomized placebo-controlled trial. *J Integr Med*. 2022;20(4):321–328. doi:10.1016/j.joim.2022.04.002
23. Wang B, Liu W, Li JJ, et al. A low dose cell therapy system for treating osteoarthritis: in vivo study and in vitro mechanistic investigations. *Bioact Mater*. 2022;7:478–490. doi:10.1016/j.bioactmat.2021.05.029
24. Flatters SJL, Bennett GJ. Studies of peripheral sensory nerves in paclitaxel-induced painful peripheral neuropathy: evidence for mitochondrial dysfunction. *Pain*. 2006;122(3):245–257. doi:10.1016/j.pain.2006.01.037
25. Pauli P, Rau H, Zhuang P, Brody S, Birbaumer N. Effects of smoking on thermal pain threshold in deprived and minimally-deprived habitual smokers. *Psychopharmacology*. 1993;111(4):472–476. doi:10.1007/bf02253538
26. Wang S, Ma ZZ, Lu YC, et al. The localization research of brain plasticity changes after brachial plexus pain: sensory regions or cognitive regions? *Neural Plast*. 2019;2019:7381609. doi:10.1155/2019/7381609
27. Xing XX, Hua XY, Zheng MX, et al. Abnormal brain connectivity in carpal tunnel syndrome assessed by graph theory. *J Pain Res*. 2021;14:693–701. doi:10.2147/JPR.S289165
28. Wang J, Wang X, Xia M, Liao X, Evans A, He Y. GRETNA: a graph theoretical network analysis toolbox for imaging connectomics. *Front Hum Neurosci*. 2015;9:386. doi:10.3389/fnhum.2015.00386
29. Otake K, Nakamura Y. Forebrain neurons with collateral projections to both the interstitial nucleus of the posterior limb of the anterior commissure and the nucleus of the solitary tract in the rat. *Neuroscience*. 2003;119(3):623–628. doi:10.1016/s0306-4522(03)00216-1
30. Shammah-Lagnado SJ, Alheid GF, Heimer L. Afferent connections of the interstitial nucleus of the posterior limb of the anterior commissure and adjacent amygdalostriatal transition area in the rat. *Neuroscience*. 1999;94(4):1097–1123. doi:10.1016/S0306-4522(99)90280-4
31. Hasue RH, Shammah-Lagnado SJ. Origin of the dopaminergic innervation of the central extended amygdala and accumbens shell: a combined retrograde tracing and immunohistochemical study in the rat. *J Comp Neurol*. 2002;454(1):15–33. doi:10.1002/cne.10420
32. Cai J, Tong Q. Anatomy and function of ventral tegmental area glutamate neurons. *Front Neural Circuits*. 2022;16:867053. doi:10.3389/fncir.2022.867053
33. Zhou Q, Womer FY, Kong L, et al. Trait-related cortical-subcortical dissociation in bipolar disorder: analysis of network degree centrality. *J Clin Psychiatry*. 2017;78(5):584–591. doi:10.4088/JCP.15m10091
34. Kuner R, Kuner T. Cellular circuits in the brain and their modulation in acute and chronic pain. *Physiol Rev*. 2021;101(1):213–258. doi:10.1152/physrev.00040.2019

35. Vertes RP, Linley SB, Hoover WB. Limbic circuitry of the midline thalamus. *Neurosci Biobehav Rev*. 2015;54:89–107. doi:10.1016/j.neubiorev.2015.01.014
36. Berridge KC, Kringelbach ML. Pleasure systems in the brain. *Neuron*. 2015;86(3):646–664. doi:10.1016/j.neuron.2015.02.018
37. Howard MA, Sanders D, Krause K, et al. Alterations in resting-state regional cerebral blood flow demonstrate ongoing pain in osteoarthritis: an arterial spin-labeled magnetic resonance imaging study. *Arthritis Rheum*. 2012;64(12):3936–3946. doi:10.1002/art.37685
38. Vuksanović V, Staff RT, Ahearn T, Murray AD, Wischik CM. Cortical thickness and surface area networks in healthy aging, Alzheimer's disease and behavioral variant fronto-temporal dementia. *Int J Neural Syst*. 2019;29(6):1850055. doi:10.1142/s0129065718500557
39. Shah C, Liu J, Lv P, et al. Age related changes in topological properties of brain functional network and structural connectivity. *Front Neurosci*. 2018;12:318. doi:10.3389/fnins.2018.00318
40. Anderson A, Cohen MS. Decreased small-world functional network connectivity and clustering across resting state networks in schizophrenia: an fMRI classification tutorial. *Front Hum Neurosci*. 2013;7:520. doi:10.3389/fnhum.2013.00520